Coverage and Capacity Analysis for Football Player's Bodycam with Cell-Free Massive MIMO

Hersyandika, Rizqi ; Rossanese , Marco ; Lutu, Andra ; Yang, Miao; Wang, Qing; Pollin, Sofie

DOI
10.1109/ICCWorkshops57953.2023.10283510

Publication date
2023

Document Version
Final published version

Published in
Proceedings of the 2023 IEEE International Conference on Communications Workshops (ICC Workshops)

Coverage and Capacity Analysis for Football Player's Bodycam with Cell-Free Massive MIMO

Rizqi Hersyandika[1], Marco Rossanese[2], Andra Lutu[3], Yang Miao[1,5], Qing Wang[4], and Sofie Pollin[1]

[1]Katholieke Universiteit Leuven, Belgium
[2]NEC Laboratories Europe, Germany
[3]Telefonica Research, Spain
[4]Delft University of Technology, the Netherlands
[5]University of Twente, the Netherlands

2023 IEEE International Conference on Communications Workshops (ICC Workshops) | 979-8-3503-3307-7/23/$31.00 ©2023 IEEE | DOI: 10.1109/ICCWORKSHOPS57953.2023.10283510

***Abstract*—This paper studies a promising use case of a private 5G network for the sports industry: wearable bodycams and sensors in a football match. This use case requires a reliable and dedicated massive MIMO network to provide uniform coverage with a high capacity in the whole pitch area. The coverage of co-located and distributed (cell-free) massive MIMO, differing in the configuration of base station antenna placement inside the stadium, are evaluated through ray tracing using a 3D stadium model and players' mobility dataset. The results give insight into how distributed antennas inside the stadium should be deployed to enhance the uniform coverage of moving wearable devices. Besides that, the uplink capacity performance and the impact of channel aging on the capacity are also evaluated. The results demonstrate the advantages and disadvantages of different base station antenna distribution strategies in terms of coverage, capacity and channel aging impact.**

***Index Terms*—massive MIMO, cell-free, coverage, channel aging, private 5G, sports**

I. Introduction

In the future, football and other sports players might be equipped with wearable on-body cameras (bodycams) and other sensors while on the pitch. The bodycam view can be utilized by the broadcaster to provide a richer experience for the viewers. The view from the player's perspective is also beneficial for the referee and match official to help them in making decisions during the game. In 2022, a friendly match between AC Milan and FC Cologne tried out the bodycam technology [1]. Each player is equipped with a bodycam and microphone, enabling attractive live action from the players' point of view. Meanwhile, wearable sensors can help the coaching team monitor the player's vital signs and track the player's movement, which will also be helpful for match analysis purposes. The referee can also use the sensor information to take a decision on the pitch, e.g. in the case of a foul or injury. The use of sensors to monitor the vital signs of football players has been studied in [2]. Several football clubs have tried using sensors to observe brain activity during training sessions. To support this use case, reliable connectivity to the pitch is necessary.

Cellular operators typically deploy their base stations in a Distributed Antenna System (DAS) fashion inside a football stadium to provide 2G, 3G, and 4G coverage for the spectators. These antennas are typically deployed on the stadium rooftop, with several sectors also covering the surrounding area. However, DAS has a capacity limitation to serve a massive number of spectators during the game. Adding more base stations will increase the interference, thus, degrading the performance. Smaller cell deployment was proposed to boost the capacity to complement the legacy DAS [3].

A data rate of 85 to 110 Mbps is required to deliver an uncompressed 8K 120-Hz video stream from the bodycam smoothly [4], which is achievable by the 5G networks. In several sports arenas, the 5G networks have been rolled out to provide the spectators with an enhanced viewing experience through Augmented Reality (AR), such as accessing live action, instant replay from multi-viewing angles and real-time match statistics [5], [6]. In addition, the integrated system involving the player and the ball tracking, AR, and 3-D camera view broadcasting supported by a private 5G network in a large sports arena has been proposed and evaluated in [7]. The experimental evaluation of the stadium's massive MIMO channel stationary behaviour has been investigated in [8].

One of the challenges in the player's bodycam and sensor application use case is the player's high mobility on the field, causing faster channel aging compared to the static or slowly moving user. The impact of channel aging on massive MIMO systems has been studied, where [9] proposes channel prediction to overcome the channel aging effects in massive MIMO, and [10] shows that a strong spatial correlation in cell-free massive MIMO reduces the channel aging effect.

This paper studies a potential use case of a private 5G network for the sports industry, particularly football, providing insight to the network operator, the sports association, and other stakeholders on how the network should be deployed for this use case. We evaluate different deployment configurations of massive MIMO networks inside the stadium through ray tracing using a 3D stadium model and players' mobility dataset. The contributions of this work are threefold:

1) We study the existing 5G gNodeB network performance in a stadium during the football match day based on the dataset of a cellular operator in the London area. It shows how the 5G network is overloaded by the spectators during the match, justifying the need for

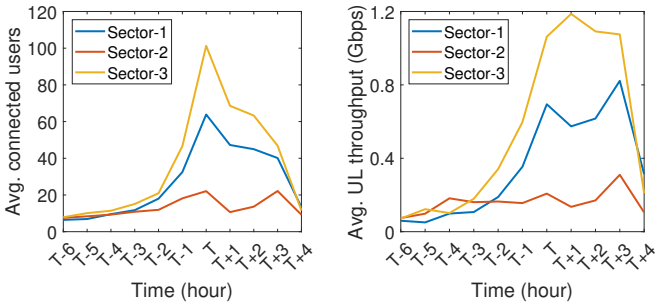

(a) Connected users (b) Uplink throughput

Fig. 1: 5G gNodeB performance in the stadium during match days

a private and dedicated network for the use case of wearable bodycam and sensors of football players.

2) Through ray-tracing-based simulations, we provide the pitch coverage analysis for different base station antenna placement configurations. The results give insight into how the base station antennas should be deployed in the stadium to provide uniform coverage on the pitch.
3) We simulate the football match with 22 mobile transceivers on the pitch using the players' mobility dataset to evaluate the achievable uplink capacity during the match. Besides that, we also analyzed the channel aging impact due to the high mobility of players.

II. System Topology, Design and Connectivity Performance Metrics

A. Coverage on the pitch

Our study on a cellular operator's 5G network performance in Stamford Bridge Chelsea stadium, London, shows that spectators overload the gNodeB in the stadium before and during the match, as shown in Fig. 1. The gNodeB is placed in one of the stadium rooftop corners. It has three sector antennas where Sector-1 partially covers the stadium, Sector-2 covers the area outside the stadium, and Sector-3 covers the seating areas inside the stadium. **T** indicates the kick-off time. Fig. 1a and Fig. 1b show the average number of connected users and the average uplink (UL) throughput of all antenna sectors averaged hourly over six different matchdays. The increasing number of connected users and UL throughput can be observed 2 hours before the kick-off time. The peak average connected users and UL throughput of Sector-3 increased to over 12.8 and 16.5 times, respectively, compared to those 6 hours before the match, showing how the network was overloaded during the match. Consequently, the wearable bodycam and sensor application cannot share the same existing public 5G network and compete with the spectators' devices. A private and dedicated network is thus required to serve this use case exclusively.

The wearable bodycam and sensor application require reliable coverage and capacity in the whole pitch area. In this use case, the User Equipment (UE) of each player on the field sends an uplink data stream containing an uncompressed video stream from the bodycam and real-time sensor data to the base stations (BSs). As the players move a lot during the game, the whole pitch area should be covered by the BSs to avoid any zone lacking coverage. As the UEs transmit the uplink streams with a fixed Tx power, the whole pitch area must be covered by uniform channel gain. This could be achieved by strategically deploying the base station antennas inside the stadium.

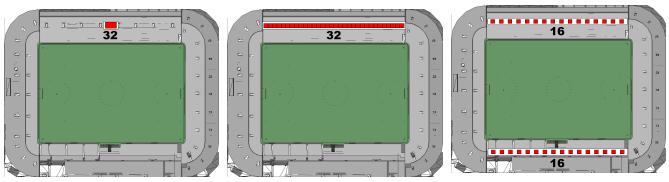

(a) Co-located (C0) (b) Distributed in one side (C1) (c) Distributed in two sides (C2)

Fig. 2: Massive MIMO antenna placement configurations

The BS antennas are placed in the frame of the stadium roof, down-tilted toward the pitch. We consider three different antenna placement configurations: C0, C1 and C2, as described in Fig. 2, in which the red squares indicate the location of BS antennas. C0 represents the co-located massive MIMO configuration, where all antennas are placed in the center of a stadium side, with half-wavelength spacing between the antennas. Meanwhile, C1 and C2 represent the distributed massive MIMO configuration. In C1, the antennas are distributed along one side of the stadium, while in C2, the antennas are distributed along both sides. By distributing the antennas throughout the environment, we expect to obtain favourable coverage condition. This condition ensures good reception for the worst locations, achieved when the mean and the minimum Rx level are relatively high [11]. Different shapes of stadiums (e.g. with an oval roof) might require different BS distribution points.

At the UE side, the antenna can be attached to the player's jersey (e.g. on the shoulder or the upper back part). The antenna design and placement need to consider the shadowing caused by the player's own body part and caused by other players. The typical body movement of players should also be taken into account. Nevertheless, the UE antenna design is not the main focus of this paper. For simplicity, we consider using an omnidirectional antenna at the UE.

We consider $M = 22$ UEs representing 22 players on the pitch and N serving BSs. The downlink signal from the n-th BS to the m-th UE on the field is expressed as:

$$\hat{y}_{mn}^{DL} = \sqrt{p_n}\hat{h}_{mn}^{DL}x_n + w_m, \quad (1)$$

where p_n is the BS transmit power, $\hat{h}_{mn}^{DL}$ is the downlink channel transfer function between the n-th BS and the m-th UE, x_n is the transmitted information by the n-th BS, and w_m is the noise at the m-th UE. Therefore, the total downlink

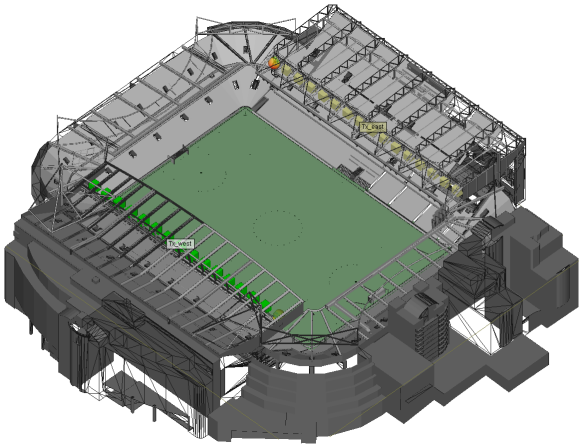

Fig. 3: Football stadium 3-D model

signal from all N base stations received by the *m*-th UE becomes:

$$y_m^{DL} = \sum_{n=1}^{N} |\hat{y}_{mn}^{DL}|^2. \tag{2}$$

B. Uplink capacity in massive MIMO

Since we consider the UE with one antenna transmitting the data stream without precoding, the uplink signal sent by the *m*-th UE and received by the *n*-th BS can be expressed as:

$$\hat{y}_{mn}^{UL} = \sqrt{p_m}\hat{h}_{mn}^{UL} x_m + w_n, \tag{3}$$

where p_m is the transmit power of the m-th UE, $\hat{h}_{mn}^{UL}$ is the uplink channel transfer function between the *m*-th UE and *n*-th BS including the antenna gain at both sides, x_m is the transmitted information by the m-th UE, and w_n is the noise at the *n*-th BS.

We consider a cell-free massive MIMO network in which a set of cooperative BSs serves all UEs at the same time-frequency domain [12]. A Central Processing Unit (CPU) coordinating all BSs collects the channel state information from each BS, obtained through the channel estimation process prior to the uplink transmission. The uplink channel matrix between all M UEs and N BSs is denoted as $\hat{\mathbf{H}} \in \mathbb{C}^{M \times N}$. Zero Forcing (ZF) combining scheme is considered for the joint processing of N base stations. The combined channel estimation $\hat{\mathbf{H}}$ is then used to determine the combining vector. In the ZF scheme, the combining vector is defined as follows [13]:

$$\mathbf{V^{ZF}} = \hat{\mathbf{H}} \left(\hat{\mathbf{H}}^{\mathbf{T}} \hat{\mathbf{H}} \right)^{-\mathbf{1}} \in \mathbb{C}^{M \times N}, \tag{4}$$

in which $\mathbf{V} = [v_{11}, \ldots, v_{MN}]$ and $\hat{\mathbf{H}}^{\mathbf{T}}$ denotes the nonconjugate transpose of $\hat{\mathbf{H}}$.

The instantaneous uplink Signal-to-Interference-plus-Noise Ratio (SINR) of transmission from the m-th UE to the n-th BS after the combining process becomes:

$$SINR_{mn}^{UL} = \frac{p_m |v_{mn}^H \hat{h}_{mn}|^2}{\sum\limits_{j \neq m}^{M} p_j |v_{jn}^H \hat{h}_{jn}|^2 + w_n^2}. \tag{5}$$

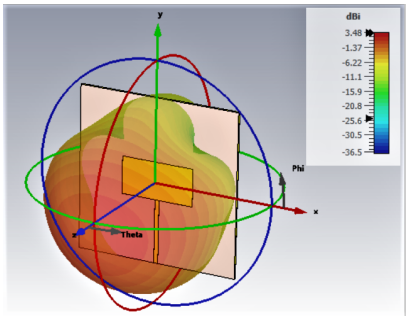

Fig. 4: Radiation pattern of 5G patch antenna at 3.5 GHz

Therefore, the uplink spectral efficiency per user becomes:

$$SE_m^{UL} = \sum_{n=1}^{N} \log_2(1 + SINR_{mn}^{UL}). \tag{6}$$

C. Simulation environment

To recreate an environment as close to reality, we selected Wireless InSite [14], a 3D ray-tracing simulator widely used in the research community to analyze site-specific radio wave propagation and wireless communication systems. The chosen propagation model is the X3D Ray Model, a full 3D propagation model with a high accuracy achieved through the exact path calculations. For our purpose, we applied a ray spacing of 10° with reflections up to the third order and one diffraction per ray.

We use a 3-D model of Stamford Bridge Chelsea stadium [15] in London, UK, as shown in Fig. 3. The model contains over 50.000 polygons with 134 different materials. We then simplified the model by grouping the elements into four main materials: 1) *concrete* with permittivity $\epsilon = 5.31$ F/m, conductivity $\sigma = 0.08987$ S/m and thickness = 30 cm for the main building and tribune, 2) *glass* with $\epsilon = 6.27$ F/m, $\sigma = 0.01915$ S/m, and thickness = 3 mm for the roof covering the tribune, 3) *grass* for the pitch area with the size of 74×109 m^2 and 4) *metal* with perfect electric conductor for the frames on the roof and other metal components.

Base station antennas are deployed on the stadium frame at 25 m above the pitch, as depicted by the green and yellow boxes in Fig. 3, pointing 60° downward from the horizon to cover the pitch. The distances between antennas in the case of 8, 16, 32, and 64 distributed antennas deployment along one frame are 12.8 m, 6.4 m, 3.2 m and 1.6 m, respectively. The base station uses a 5G patch antenna at the 3.5 GHz band designed with CST Studio. The antenna contains a 2-layered PCB with a standard FR-4 substrate of a thickness of 1.13 mm covered by two layers of copper 0.035 mm thick. The patch size is 38.4 mm $\times$ 19.5 mm, and the ground layer is 85.4 mm $\times$ 85.4 mm, whose length corresponds to $\lambda/2$ of the operating frequency. The 5G patch antenna pattern is depicted in Fig. 4, showing a gain of 3.48 dBi at the desired frequency. On the other side, each UE uses an omnidirectional antenna with a height of 2 m above the pitch.

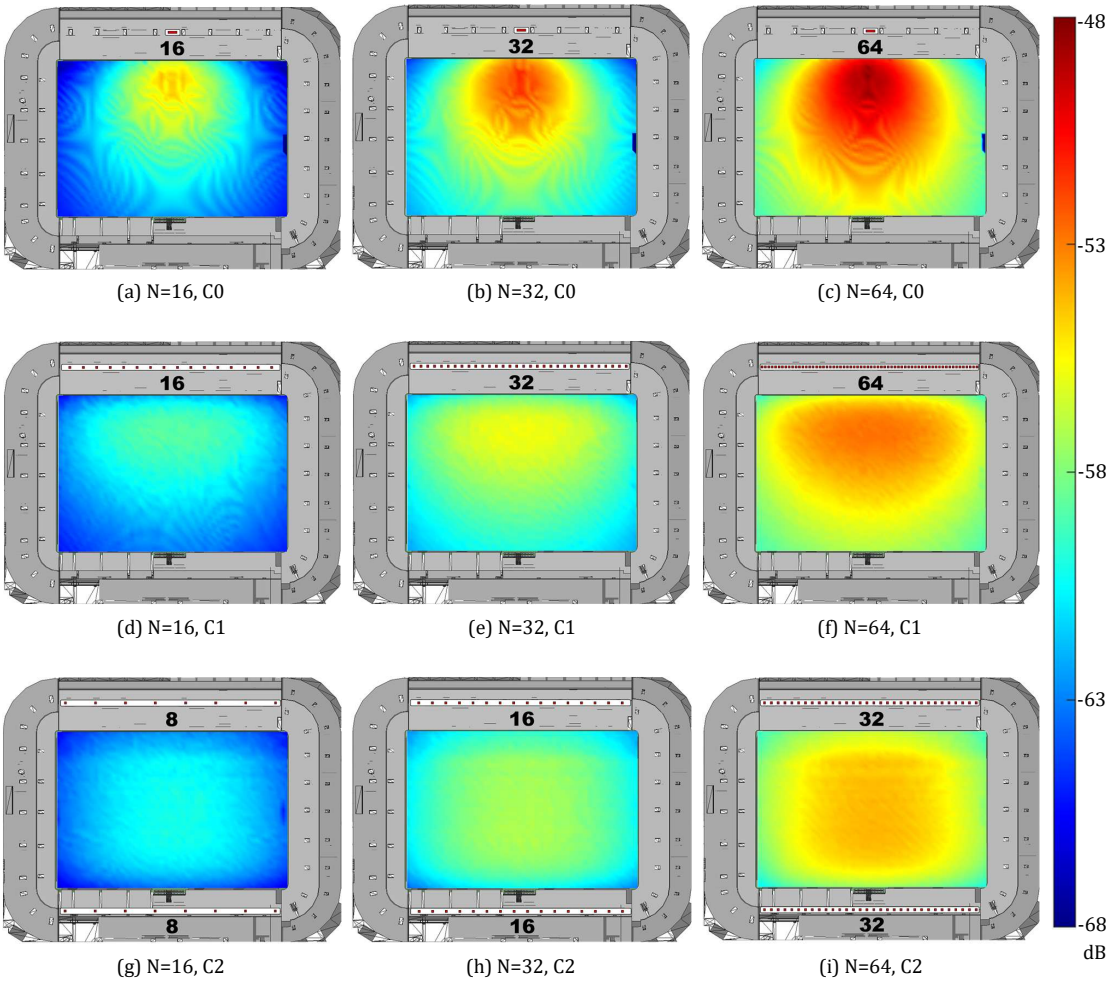

Fig. 5: Channel gain for different antenna configurations

We consider a carrier frequency of 3,510 MHz with 20 MHz bandwidth. The noise figure is assumed to be 7 dB in both BS and UE. The total Tx power of 43 dBm is shared equally among all BS antennas. We consider a downlink transmission from BS to UE in all simulations and assume the uplink-downlink channel reciprocity.

1) Coverage simulation: For the coverage analysis, we consider downlink transmission from all BSs to all Rx points on the pitch, distributed in a grid sized 37×54 with a 2 m spacing. Ray tracing is performed to obtain the downlink channel between each BS and Rx point. The different numbers of BS antennas: $N = 16$, 32 and 64, with various configurations: C0, C1 and C2, are simulated. The total received signal power from all BS antennas in each Rx point is calculated using Eq. (2).

2) Uplink capacity simulation: This simulation aims to analyze the uplink capacity of transmission from players on the pitch to base stations. A football game is simulated based on the football players' tracking dataset from [16]. The dataset contains the actual positions of all players on the pitch during an entire match sampled every 40 ms. The player's movement is only represented by the translation between points since the information about the player's body orientation and rotation are not available on the dataset. For the simulation, we sampled the players' positions every 10 s during the first half of a match, resulting in 271-time samples. For each time sample, the static channel state information from $M = 22$ players to all N base station antennas are acquired to generate $\hat{\mathbf{H}} \in \mathbb{C}^{M \times N \times 271}$.

3) Channel aging simulation: The objective of this simulation is to observe the channel aging impact on uplink capacity. The players' tracking dataset [16] containing players' positions per 40 ms period are interpolated to generate the players' positions per 1 ms. This small-scale movement is simulated to obtain the static channel state information every 1 ms interval during a 40 ms period.

III. Results and Analysis

A. Coverage uniformity

Fig. 5 describes the coverage, represented by the channel gain, in the whole pitch area for different numbers of BS antennas with various configurations. The channel gain is obtained through the total downlink signal from all base

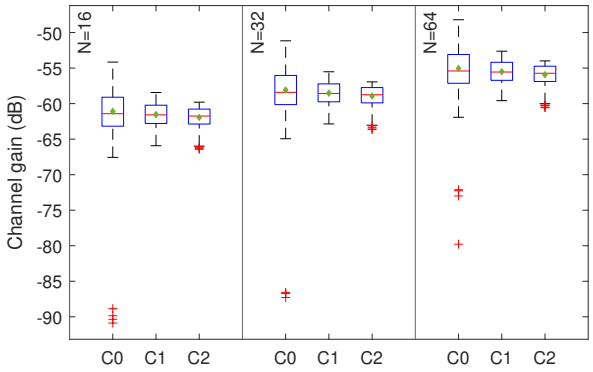

Fig. 6: Channel gain distribution

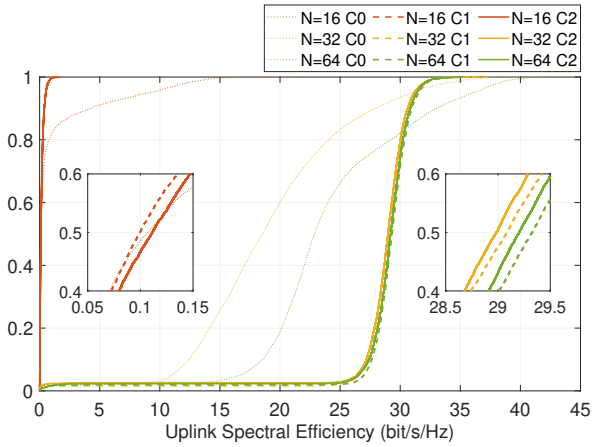

Fig. 7: Capacity performance

stations normalized by the BS's Tx power. Co-located massive MIMO (C0) is shown to provide the maximum achievable channel gain among all configurations. The highest channel gain is concentrated at the center of the pitch following the BS antenna placement. However, this configuration doesn't provide uniform coverage since the corner areas have a significantly low channel gain. By placing the BS antennas along one tribune side, as in C1, the channel gains are more distributed in the areas near the upper tribune. The channel gains are distributed more uniformly in almost all areas by allocating half of the total number of BS antennas on both sides of the stadium, as in C2, with the cost of lowering the achievable maximum channel gain.

Fig. 6 shows the channel gain distribution on the whole pitch area. In each size N, the average channel gains of different configurations, as indicated by the green diamond, are comparable. However, the minimum channel gain of C0 is significantly lower than other configurations, i.e., lower than -90 dB in the worst locations as indicated by the red outlier marks. Meanwhile, C1 and C2 have the minimum channel gain of -65.9 dB and -66.4 dB, respectively. It demonstrates how the distribution antenna configuration provides more favourable coverage conditions than the co-located one. The largest variation of channel gain is also observed in C0. The total Rx power standard deviation values for each configuration in all N sizes are displayed in Table I, where C2 provides the least standard deviation value among all configurations. Therefore, coverage uniformity can be achieved by distributing BS antennas, particularly with the C2 configuration.

B. Uplink capacity

In the uplink capacity analysis, the ZF combining scheme is considered. Fig. 7 shows the Cumulative Distribution Function (CDF) of uplink spectral efficiency for different numbers of BS antennas with various configurations. When using 16 BS antennas, C0 provides better spectral efficiency for around 46% of the locations than C1 and C2. C1 and C2 have similar spectral efficiency performances, where the maximum achievable spectral efficiency by both configurations is only 1.735 bit/s/Hz. In general, the spectral efficiency performance with 16 BS antennas is worse than others with 32 and 64 BS antennas because the CPU does not have full-rank channel knowledge of all 22 players on the pitch. Other sports with different numbers of players might require different numbers of BS units.

TABLE I: Std. dev. of Total Rx power (μW)

Config./Ant.	N=16	N=32	N=64
C0	13.9	27.2	54.2
C1	5.4	10.8	21.5
C2	**3.8**	**7.5**	**15.1**

Adding more BS antennas to 32 and 64 improves the spectral efficiency significantly. In the case of C0, the spectral efficiency gap between using 32 and 64 BS antennas is clearly visible in Fig. 7, showing the advantage of array gain in this configuration. With C0, the maximum achievable spectral efficiency of 41.6 and 44.2 bit/s/Hz can be achieved by $N = 32$ and $N = 64$, respectively. Nevertheless, in the football player's bodycam scenario, the uniform capacity for all players matters more than the maximum capacity achieved by a small number of players in specific locations on the field. In C0, players achieve more than 25 bit/s/Hz in 17% and 44% of the cases when using $N = 32$ and $N = 64$, respectively. Meanwhile, with C1 and C2, more than 25 bit/s/Hz can be achieved in 99.7% of the cases, showing the huge benefit of spatially distributed massive MIMO configurations in providing better uniform coverage on the field during the game.

Fig. 7 also shows that by using either C1 or C2, increasing the BS antennas from 32 to 64 only improves the spectral efficiency by 0.2 bit/s/Hz. It indicates that using $N = 32$ is preferred over $N = 64$ for this use case, considering the deployment and operational cost of a larger number of BS units. For the same number of BS antennas, C1 has a slight spectral efficiency advantage of 0.1 bit/s/Hz higher than C2.

C. Channel aging impact

The high mobility of football players makes the channel age quickly. From the football players' tracking dataset, the average player speed is 2.045 m/s. Thus, the coherence time

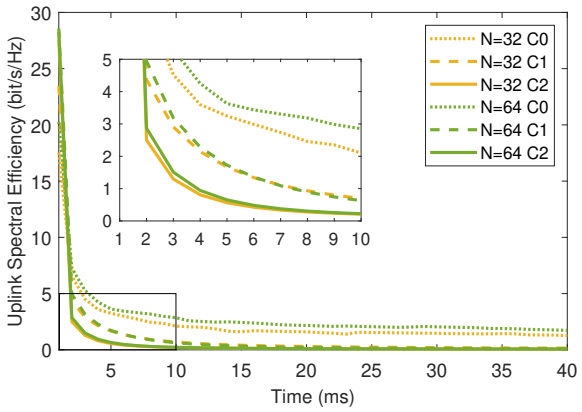

Fig. 8: Channel aging impact

at 3.5 GHz becomes 41.9 ms. We use the channel estimation obtained at $t = 0$ ms to create the ZF combining vector and use it to calculate the uplink spectral efficiency during the next 40 ms with a 1 ms interval.

Fig. 8 shows the degradation of uplink spectral efficiency resulting from the channel aging in the case of $N = 32$ and $N = 64$. The spectral efficiency degrades significantly already after 1 ms due to a resulting high channel estimation error in the ZF combining. For the same configuration, the decreasing slopes are similar regardless of the size N, except in the case of C0, where the spectral efficiency of $N = 64$ degrades slower than $N = 32$. The spectral efficiency reaches below 1 bit/s/Hz after 8 ms and 4 ms with C1 and C2, respectively. Meanwhile, C0 can maintain its spectral efficiency above 1 bit/s/Hz during the 40 ms period. It shows the drawback of distributed massive MIMO configuration in channel aging compared to the co-located one.

IV. Conclusion

This paper investigates a potential use case of a private 5G network for the football industry, where the performance of co-located vs distributed massive MIMO implementation inside the stadium to serve the wearable bodycam and sensor application is evaluated. Various BS antenna placement configurations with different numbers of antennas are deployed in a football stadium to serve the uplink stream from the players on the pitch. The required coverage uniformity for this use case is achieved by having distributed BS antennas. The uplink capacity during the game is analyzed based on the player's position during the real football game, where the distributed massive MIMO configuration outperforms the co-located one. Besides that, the impact of channel aging due to players' mobility on capacity performance is also evaluated. The results show that the spectral efficiency in the distributed massive MIMO configuration degrades faster than in the co-located one. Therefore, to achieve uniform coverage and capacity, and to alleviate the channel aging impact, a distributed or cell-free massive MIMO configuration with more frequent channel estimation is required. Future work can investigate the channel estimation strategy to cope with the high mobility of the players, the self-blockage impact, the optimal antenna placement on the player's jersey and other requirements, such as end-to-end latency.

Acknowledgment

This work has received funding from the European Union's Framework Programme for Research and Innovation Horizon 2020 under Grant Agreement No. 861222 (MINTS project).

References

[1] StartupHub.ai, "FC Cologne – AC Milan Football Match to Feature MindFly AI-Powered Bodycam to Give Fans Player's Perspective," 2022. [Online]. Available: https://www.startuphub.ai/1-fc-cologne-ac-milan-football-match-to-feature-mindfly-ai-powered-bodycam-to-give-fans-players-perspective/

[2] S. Hara, T. Tsujioka, T. Shimazaki, K. Tezuka, M. Ichikawa, M. Ariga, H. Nakamura, T. Kawabata, K. Watanabe, M. Ise, N. Arime, and H. Okuhata, "Elements of a real-time vital signs monitoring system for players during a football game," in *2014 IEEE 16th International Conference on e-Health Networking, Applications and Services (Healthcom)*, 2014.

[3] Ericsson, "Connected stadiums - connected fans," 2022. [Online]. Available: https://www.ericsson.com/en/small-cells/stadium

[4] Y. Sugito, S. Iwasaki, K. Chida, K. Iguchi, K. Kanda, X. Lei, H. Miyoshi, and K. Kazui, "A Study on the Required Video Bit-rate for 8K 120-Hz HEVC/H.265 Temporal Scalable Coding," in *2018 Picture Coding Symposium (PCS)*, 2018.

[5] GSMA, "How 5G is transforming sports for spectators," 2022. [Online]. Available: https://www.gsma.com/5GHub/stadiums

[6] Nokia, "How 5G and private networks are making stadiums smarter and events more engaging," 2022. [Online]. Available: https://www.nokia.com/blog/how-5g-and-private-networks-are-making-stadiums-smarter-and-events-more-engaging/

[7] C.-W. Wu, M.-D. Shieh, J.-J. J. Lien, J.-F. Yang, W.-T. Chu, T.-H. Huang, H.-C. Hsieh, H.-T. Chiu, K.-C. Tu, Y.-T. Chen, S.-Y. Lin, J.-J. Hu, C.-H. Lin, and C.-S. Jheng, "Enhancing Fan Engagement in a 5G Stadium With AI-Based Technologies and Live Streaming," *IEEE Systems Journal*, 2022.

[8] L. Liu, C. Tao, D. W. Matolak, Y. Lu, B. Ai, and H. Chen, "Stationarity Investigation of a LOS Massive MIMO Channel in Stadium Scenarios," in *2015 IEEE 82nd Vehicular Technology Conference (VTC2015-Fall)*, 2015.

[9] K. T. Truong and R. W. Heath, "Effects of channel aging in massive MIMO systems," *Journal of Communications and Networks*, 2013.

[10] J. Zheng, J. Zhang, E. Björnson, and B. Ai, "Impact of Channel Aging on Cell-Free Massive MIMO Over Spatially Correlated Channels," *IEEE Transactions on Wireless Communications*, 2021.

[11] A. P. Guevara, S. De Bast, and S. Pollin, "Weave and Conquer: A Measurement-based Analysis of Dense Antenna Deployments," in *ICC 2021 - IEEE International Conference on Communications*, 2021.

[12] H. Q. Ngo, A. Ashikhmin, H. Yang, E. G. Larsson, and T. L. Marzetta, "Cell-Free Massive MIMO Versus Small Cells," *IEEE Transactions on Wireless Communications*, vol. 16, no. 3, pp. 1834–1850, 2017.

[13] E. Björnson, J. Hoydis, and L. Sanguinetti, "Massive MIMO networks: Spectral, energy, and hardware efficiency," *Foundations and Trends® in Signal Processing*, 2017.

[14] Remcom, "Wireless InSite - 3D Wireless Prediction Software," 2022. [Online]. Available: https://www.remcom.com/wireless-insite-em-propagation-software

[15] A. Zuniga, "3D Warehouse - Stamford Bridge, Chelsea," 2022. [Online]. Available: https://3dwarehouse.sketchup.com/model/c9d775844788d81cbe93ee925f0c0d10/Stamford-Bridge-Chelsea

[16] Metrica-Sports, "Football Data Analytics - Play by Metrica Sports," 2022. [Online]. Available: https://metrica-sports.com/football-data-analytics/